THE SELF-MOTIONS OF A FULLEROID-LIKE-MECHANISM

Otto RÖSCHEL
Graz University of Technology, Austria

ABSTRACT: We consider one of the Fulleroid-like mechanisms described by G. KIPER [2] and K. WOHLHART [8]. Due to the generation of this mechanism G. KIPER and K.WOHLHART worked out a highly symmetric one-parametric self-motion $\xi_0(t)$ of the mechanism and displayed some of the states of this motion. This mechanism consists of 24 rigid bodies linked via 24 rotational linkages (socalled 1R-joints) and 12 linkages, each consisting of 2 orthogonally intersecting rotational axes (socalled spherical 2R-joints). For the Fulleroid-like mechanism the theoretical degree of freedom takes on the value *F = -30*. As it admits the self-motion $\xi_0(t)$ it is an example of an overconstrained mechanism and as such of high interest. But surprisingly, a physical model of this highly over-constrained mechanism seems to admit more possible self-motions than $\xi_0(t)$! In this paper we elucidate this fact and give a complete list of the possible non-trivial self-motions of this mechanism: We will demonstrate that in general there are 4 different one-parametric non-trivial self-motions of this mechanism: The described motion $\xi_0(t)$ and 3 further motions $\xi_1(t)$, $\xi_2(t)$ and $\xi_3(t)$. They share common singular positions where bifurcations are possible. These singular positions will also be described in the paper.

Keywords: Kinematics, Robotics, Fulleroid-like-mechanisms, Overconstrained Mechanisms, Self-Motions.

…………………………………………………………………………………………………....

1. INTRODUCTION

We start with one of the Fulleroid-like mechanisms described by G. KIPER [2] and K. WOHLHART [8] (displayed in figure 1). It belongs to a class of interesting overconstrained mechanisms described by several authors (e.g. H. STACHEL [6], [7], K. WOHLHART [8], [9], G. KIPER [1], [2] and the author [3], [4], [5]). This particular example consists of six congruent parallel four-bars in the faces of a cube which are interlinked by spherical 2R-joints (at fixed angle of 90 degrees). Due to the generation of this mechanism G. KIPER and K.WOHLHART worked out a highly symmetric one-parametric self-motion $\xi_0(t)$ of the mechanism and displayed some of the states of this motion.

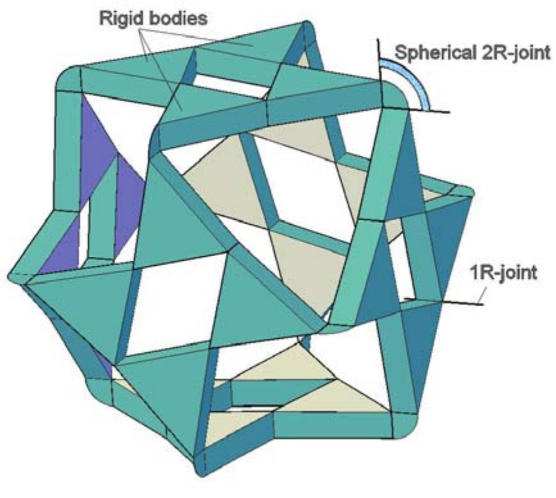

Figure 1: The basic Fulleroid-Like-Mechanism.

It consists of 24 rigid bodies linked via 24 rotational linkages (socalled 1R-joints) and 12 linkages, each consisting of 2 orthogonally intersecting rotational axes (socalled spherical 2R-joints). The theoretical degree of freedom F of such a linkage is determined via the GRÜBLER-KUTZBACH formula. It counts number of theoretical restrictions of the mechanism with respect to the number of rigid bodies. For the Fulleroid-like mechanism it takes on the value F = -30. As it admits at least $\xi_0(t)$ it is an example of an overconstrained mechanism. In the following we will determine all non-trivial self-motions of this mechanism.

The paper is structured as follows: Section 2 is devoted to the study of some properties of planar parallel four-bars which are used in chapter 3. We provide the conditions for movability. Section 4 lists the possible non-trivial self-motions of the physical model presented in figure 1. These self-motions are displayed by point paths of a characteristic point. A conclusion will round off the paper.

2. THE SPECIAL PLANAR PARALLEL 4-BAR MOTION

As the mechanism consists of interlinked 4-bars, we start our considerations with a parallel 4-bar with equal side lengths and congruent offsets built of isosceles triangles. We use a Cartesian frame $\{O x_1, y_1, z_1\}$ and the notations of figure 2. We parametrize the paths of the
points $B_i(t)(i=1,...,4)$ via

$$\begin{aligned}
B_1(t) &= (\cos t+\beta \sin t, \sin t+\beta \cos t)\\
B_2(t) &= (-\cos t-\beta \sin t, \sin t+\beta \cos t)\\
B_3(t) &= (-\cos t-\beta \sin t, -\sin t-\beta \cos t)\\
B_4(t) &= (\cos t+\beta \sin t, -\sin t-\beta \cos t)
\end{aligned} \qquad (1)$$

with $\beta \in \Re - \{0\}, t \in [-\pi, +\pi)$. This special four-bar can run in two different ways: a parallel mode described above and an anti-parallel mode. As the physical model stays in one of these modes, we will restrict our considerations to the *parallel four-bar* described in (1).

Depending upon the choice of β the points $B_i(t)$ will form a rectangle (for $\beta = \pm 1$ it is a square) with side lengths depending on *t*. Its side lengths are

$$\begin{aligned}
l_1(t) &= \overline{B_1(t)B_2(t)} = 2(\cos t+\beta \sin t)\\
l_2(t) &= \overline{B_1(t)B_4(t)} = 2(\sin t+\beta \cos t)
\end{aligned} \qquad (2)$$

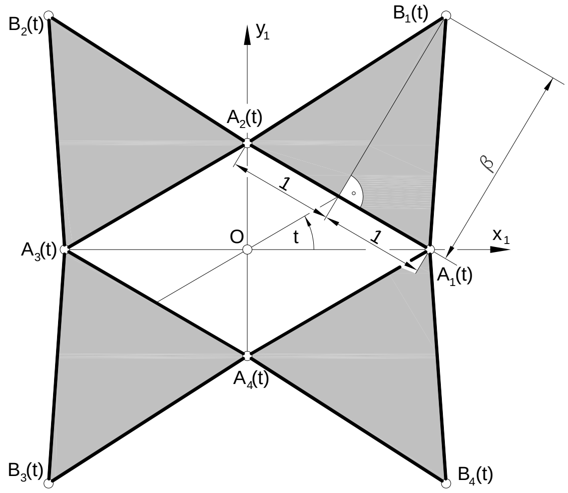

Figure 2: The basic symmetric planar parallel 4-bar.

Remarks:

1. For all $t \in [-\pi, +\pi)$ the configurations $B_i(t)$ and $B_i(t+\pi)$ are congruent via a rotation with center *O*.
2. The configurations for *t* and fixed β are congruent to those for $\pi - t$ and $-\beta$.

This allows us to restrict our considerations to $t \in [-\pi/2, +\pi/2)$ and $\beta \in \Re^+$.

3. The lengths $l_1(t)$ and $l_2(t)$ from (2) interchange if we substitute *t* by $\pi/2 - t$.

point. A conclusion will round off the paper.

3. THE LINKED PARALLEL 4-BARS

The Fulleroid-like structure is based on interlinked 4-bars. These 4-bars are positioned in 6 planes (pairwise orthogonal). They form a box with right angles at any possible position of the mechanism. We will use a global Cartesian frame $\{O; x, y, z\}$ associated with
the box, 2*a*, 2*b*, 2*c* $\in \Re^+$ being its dimensions

in the *x*, *y* and *z* direction. Figure 3 exhibits the situation.
The 4-bars in parallel (opposite) faces of the box are congruent in any position. A rotation through 180° about one of the two coordinate axes parallel to the corresponding face transforms them into each other.

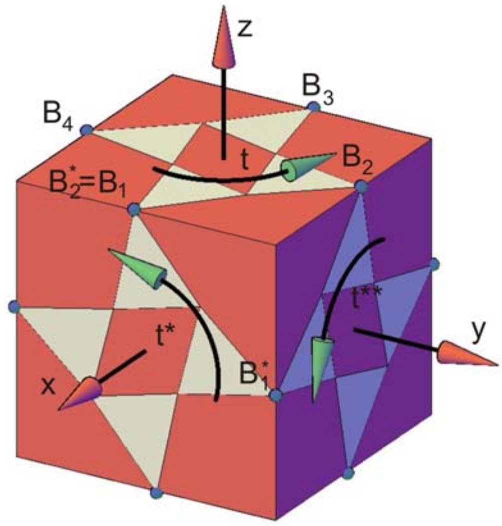

Figure 3: Schematic sketch of the box and the planar parallel 4-bars with $\beta = 2$.

For that reason it is sufficient to parametrize 3 (non-parallel) 4-bars by rotational angles *t*, *t**, *t*** (in the planes $z = \pm c, x = \pm a$ and $y = \pm b$ - see figure 3).
We have $B_1(a, y, c), B_2 = (x, b, c)$ and $B_4 = (-x, -b, c)$ with suitable values *x*, *y*, *z* $\in \Re$.
As we saw before the points B_i belong to a rectangle (with size depending on *t*). These points have the same (but not constant) distance from the center of the box. The same holds for the other facets of the box. So the linkage points on the edges of the box have to be situated on a sphere centered in the center of the box. With $\rho \in \Re^+$ denoting its radius, we have the following 3 conditions

$$
\begin{aligned}
x^2 + b^2 + c^2 &= \rho^2 \\
a^2 + y^2 + c^2 &= \rho^2 \\
a^2 + b^2 + z^2 &= \rho^2
\end{aligned}
\tag{3}
$$

Due to equation (2) and the denotations of figure 3 we have

$$
\begin{aligned}
l_1^2 = (a - x)^2 + (b - y)^2 &= 4(\cos t + \beta \sin t)^2 \\
(b - y)^2 + (c - z)^2 &= 4(\cos t^* + \beta \sin t^*)^2 \\
(a - x)^2 + (c - z)^2 &= 4(\cos t^{**} + \beta \sin t^{**})^2
\end{aligned}
\tag{4}
$$

and

$$
\begin{aligned}
l_2^2 = (a + x)^2 + (b + y)^2 &= 4(\sin t + \beta \cos t)^2 \\
(b + y)^2 + (c + z)^2 &= 4(\sin t^* + \beta \cos t^*)^2 \\
(a + x)^2 + (c + z)^2 &= 4(\sin t^{**} + \beta \cos t^{**})^2
\end{aligned}
\tag{5}
$$

Self-motions of the mechanism belong to solutions of (3), (4) and (5) for the variables *a*, *b*, *c*, *x*, *y*, *z*, *t*, *t**, *t*** and ρ all depending on at least one parameter. It is easy to compute *a*, *b*, *c*, *x*, *y*, *z* (depending of ρ, *t*, *t**, *t***) from these equations:

$$
\begin{aligned}
a^2 &= \rho^2 - (1 + \beta^2 + 2\beta \sin 2t^*) \\
b^2 &= \rho^2 - (1 + \beta^2 + 2\beta \sin 2t^{**}) \\
c^2 &= \rho^2 - (1 + \beta^2 + 2\beta \sin 2t) \\
x^2 &= 2(1 + \beta^2) + 2\beta(\sin 2t + \sin 2t^{**}) - \rho^2 \\
y^2 &= 2(1 + \beta^2) + 2\beta(\sin 2t^* + \sin 2t) - \rho^2 \\
z^2 &= 2(1 + \beta^2) + 2\beta(\sin 2t^{**} + \sin 2t^*) - \rho^2
\end{aligned}
\tag{6}
$$

Short computation yields ρ depending on *t*, *t**, *t*** given by

$$
\begin{aligned}
2\rho^2 &= \\
&= 3(1 + \beta^2) + 2\beta(\sin 2t + \sin 2t^* + \sin 2t^{**}) \pm \\
&\pm \{[1 + \beta^2 + 2\beta(\sin 2t - \sin 2t^* + \sin 2t^{**})]^2 - \\
&- (\beta^2 - 1)^2 (\cos 2t - \cos 2t^* + \cos 2t^{**})^2 \}^{1/2}
\end{aligned}
\tag{7}
$$

and the following two equations interlinking *t*, *t**, *t***:

$$2\beta(1+\beta^2+2\beta\sin 2t)(\sin 2t^{**}-\sin 2t^*)=$$
$$=(\beta^2-1)^2\cos 2t\,(\cos 2t^{**}-\cos 2t^*),$$
$$2\beta(1+\beta^2+2\beta\sin 2t^*)(\sin 2t-\sin 2t^{**})=$$
$$=(\beta^2-1)^2\cos 2t^*\,(\cos 2t-\cos 2t^{**}) \qquad (8)$$

As we have 2 equations for the 3 parameters *t*, *t**, *t*** we can expect at least one-parametric mobility of the mechanism. Further on we work out the different options for self-motions determined by (8).

4. PARAMETRISATIONS OF THE MECHANISM'S SELF-MOTIONS

We substitute $u := \tan t$, $u^* := \tan t^*$ and $u^{**} := \tan t^{**}$ in formula (8), use the abbreviation

$$C(p,q,r):=$$
$$=2\beta(1-qr)[(1+\beta^2)(1+p^2)+4\beta p]+ \qquad (9)$$
$$+(\beta^2-1)^2(1-p^2)(q+r)$$

and get the two equations

$$(u^{**}-u^*)\;C(u,u^*,u^{**})=0$$
$$(u-u^{**})\;C(u^*,u^{**},u)=0. \qquad (10)$$

The solutions of these equations belong to one of the following 4 cases:

Case A: $u = u^* = u^{**}$
Case B: $u^* = u^{**} \neq u$ and $C(u^*,u^*,u)=0$
Case C: $u = u^{**} \neq u^*$ and $C(u,u^*,u)=0$.
Case D: $u \neq u^{**}$ and $u^* \neq u^{**}$, but $C(u^*,u^{**},u)=0$ and $C(u,u^*,u^{**})=0$.

We study the 4 cases in detail:

Case A gives the very symmetric self-motion of the mechanism which was already considered by K. WOHLHART [8] and G. KIPER [2].

Case B: $u^* = u^{**}$. The second condition $C(u^*,u^*,u)=0$ allows to compute

$$u=\frac{A(u^*)}{B(u^*)} \qquad (11)$$

with the abbreviations

$$A(u^*):=2\beta[(1+\beta^2)(1+u^{*2})+4\beta u^*]+$$
$$+u^*(\beta^2-1)^2(1-u^{*2}) \qquad (12)$$
$$B(u^*):=2\beta u^*[(1+\beta^2)(1+u^{*2})+4\beta u^*]-$$
$$-(\beta^2-1)^2(1-u^{*2}).$$

In the parameter space $\{u,u^*,u^{**}\}$ this curve describes a rational quartic curve in the plane $[u^*,u^{**}]$.

Case C: $u = u^{**}$ and $C(u,u^*,u)=0$ yield a case symmetric to case B. We get

$$u^*=\frac{A(u)}{B(u)} \qquad (13)$$

with *A(u)* and *B(u)* from (10).

Case D: $u \neq u^{**}$ and $u^* \neq u^{**}$, but $C(u^*,u^{**},u)=0$ and $C(u,u^*,u^{**})=0$.
These two equations are linear in u^{**} and symmetric with respect to u and u^*. They can be solved directly, yielding the following solutions:

Case D1: $u = u^*$. This case is similar to the cases B and C. We get

$$u^{**}=\frac{A(u)}{B(u)} \qquad (14)$$

with *A(u)* and *B(u)* from (12).

Case D2: $u \neq u^*$. A careful discussion of the different cases gets us to the following result: In case D2 there are no real solutions for self-motions.

We can sum up:

Theorem 1: *The non-trivial self-motions of the Fulleroid-like-mechanism belong to two different types: The first type can be parametrized by $u=u^*=u^{**}$, the second by $u=u^*$ and $u^{**} = A(u)/B(u)$. Cyclic permutation of $\{u,u^*,u^{**}\}$ yield 2 further self-motions congruent to the second one. They parametrize rational planar quartic curves.*

All the 4 curves representing the 4 different self-motions of the mechanism share joint positions which are given by $u \in \{-1,+1,-\beta,-1/\beta\}$. Figure 4 illustrates the different options in the *(u, u*, u**)*-space which can be viewed as a parameter space of the motions. For the example we used the dimensions of figure 3 ($\beta=2$). All 4 one-parametric self-motions have the 4 common positions for $u \in \{-2,-1,-1/2,1\}$ denoted by small spheres. They are singular positions of the mechanism. This is, where bifurcations are possible.

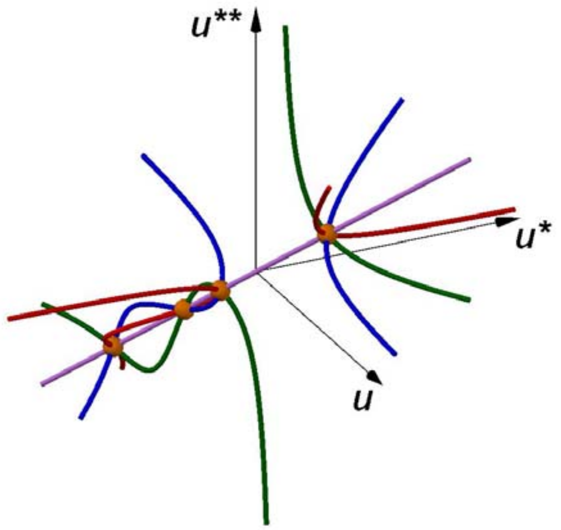

Figure 4: The self-motions for $\beta=2$ displayed as curves in the parameter space – different colors represent different self-motions.

The *special case* $\beta^2=1$ is indeed remarkable: We have only two singular positions, each of them being counted twice. For $\beta^2 \neq 1$ we have 4 real singular positions of the mechanism. We sum up:

Theorem 2: *The Fulleroid-like-mechanism in general has 4 different singular positions in the space of the parameters {u,u*,u**}. At all these positions the mechanism can branch into any of the 4 different one-parametric self-motions of theorem 1.*

5. CHARACTERISTIC POINT PATHS UNDER THE SELF-MOTIONS OF THE MECHANISM

We will visualize the different self-motions by characteristic point paths in the world-coordinates of chapter 3. Representative points are the centers of the 2R-linkages (the points B_i of figure 3). These 12 points are situated on the edges of the box. As stated before, the point paths to these points on parallel edges of the box are congruent. Therefore one self-motion will generate up to 3 different characteristic point paths. It will be sufficient to study the point paths of the 3 points $B_1, B_2, B_1{*}$.

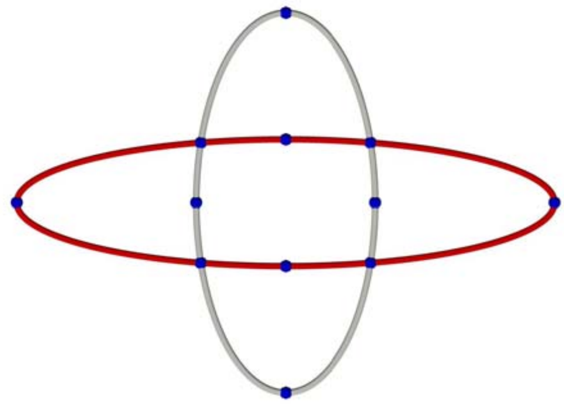

Figure 5: The point path of the point $B_1(a,y,c)$ under the self-motions of type A.

Again we have to discuss the 4 different cases:

Case A: *u = u* = u***. As we assumed $t,t*,t** \in [-\pi/2,\pi/2)$ we have *t = t* = t***. The point paths to all characteristic points are congruent. Formulae (6) and (7) then yield

$$\begin{aligned} 2\rho^2 &= 3 \pm 2\beta + 3\beta^2 \pm (1 \pm 6\beta + \beta^2)\sin 2t \\ 2a^2 &= 2b^2 = 2c^2 = (1 \pm \beta)^2 (1 \pm \sin 2t)^2 \\ 2x^2 &= 2y^2 = 2z^2 = (1 \mp \beta)^2 (1 \mp \sin 2t)^2 \end{aligned} \tag{15}$$

The path of the characteristic point $B_1(a,y,c)$ is displayed in figure 5 for $\beta=2$. We get two ellipses (belonging to the different signs in (15) – the one belonging to the lower sign is illustrated in grey color).

The bifurcation points are represented by small spheres again.

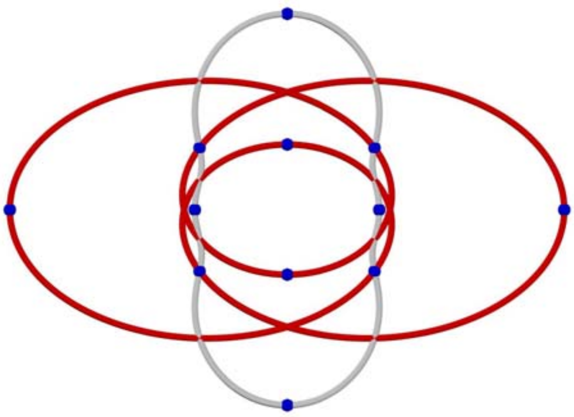

Figure 6: The point path of the point B_1 under the self-motions of type D.

The 3 **Cases B-D** deliver congruent self-motions. Their description is gained by from one by careful permutation of the coordinates and the parameters. The 12 characteristic points define 3 quadruples (stemming from parallel edges of the box) – each of it delivering congruent point paths. As representative we can consider the points $\{B_1, B_2, B_1^*\}$ (see figure 3) and their paths. These paths generated by one of these self-motions are congruent to those of these 3 points under the other self-motions, but in different ordering of the triple $\{B_1, B_2, B_1^*\}$. We start our discussions with

Case D: We have *u=u**. Formulae (6) and (7) then yield

$$\begin{aligned} &2\rho^2 = \\ &= 2(1+\beta^2)+4\beta \sin 2t + (1\pm\beta)^2(1\pm \sin 2t^{**}) \\ &2a^2 = 2c^2 = (1\pm\beta)^2(1\pm \sin 2t) \qquad (16) \\ &2b^2 = 4\beta(\sin 2t - \sin 2t^{**}) + (1\pm\beta)^2(1\pm \sin 2t^{**}) \\ &2x^2 = 2z^2 = (1\mp\beta)^2(1\mp \sin 2t) \\ &2y^2 = 2(1+\beta^2)+4\beta \sin 2t - (1\pm\beta)^2(1\pm \sin 2t^{**}) \end{aligned}$$

The parameters *t* and *t*** are interlinked via formula (14) with *u = tan t*, *u** = tan t***. The point path of the point B_1 is planar. It consists of two algebraic curves (belonging to the 2 different solutions for ρ). Figure 6 illustrates this situation for $\beta = 2$.

The point paths of the point B_1 under the self-motions of type A and D are coplanar and are tangent or intersect. The singular positions are denoted by small spheres. One curve of each type (the upper sign in formulae (15) and (16)) yield figure 7.

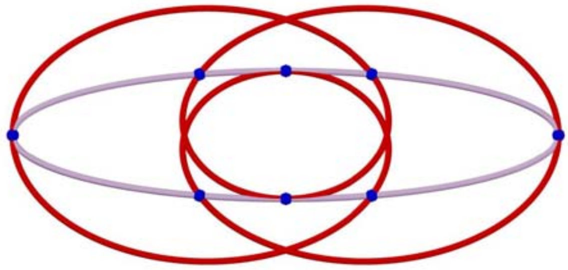

Figure 7: One part of the point paths of B_1 under the self-motions of type A and D.

Cases B and C: We either have *u*=u*** or *u** = u*. Permutations of *{a,b,c}*, *{x,y,z}* and *{t,t*,t**}* yield parametrisations to the point path of B_1. For Case B we have $\tan t = u = A(\tan t^*)/B(\tan t^*)$ and get

$$\begin{aligned} &2\rho^2 = \\ &= 2(1+\beta^2)+4\beta \sin 2t^* + (1\pm\beta)^2(1\pm \sin 2t) \\ &2a^2 = (1\pm\beta)^2(1\pm \sin 2t) \qquad (17) \\ &2c^2 = 4\beta(\sin 2t^* - \sin 2t) + (1\pm\beta)^2(1\pm \sin 2t) \\ &2y^2 = (1\mp\beta)^2(1\mp \sin 2t). \end{aligned}$$

Case C with $u = u^{**}$ and $\tan t^* = u^* = A(\tan t)/B(\tan t)$ yields

$$\begin{aligned} &2a^2 = 4\beta(\sin 2t - \sin 2t^*) + \\ &\quad + (1\pm\beta)^2(1\pm \sin 2t^*) \qquad (18) \\ &2y^2 = (1\mp\beta)^2(1\mp \sin 2t^*) \\ &2c^2 = (1\pm\beta)^2(1\pm \sin 2t^*). \end{aligned}$$

So these point paths of Case B and Case C are congruent (reflection in the plane *x+z=0*). Figure 8 shows the characteristic point paths for Case B (again for $\beta = 2$). The path consists of 4 algebraic curves.

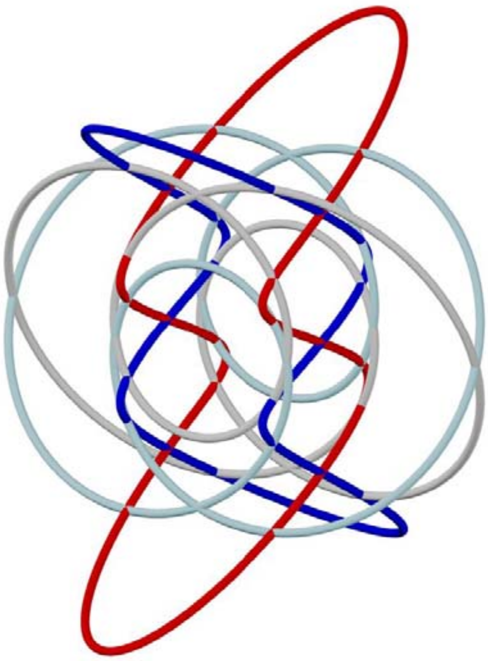

Figure 8: The point path of the point B_1 under the self-motions of Cases B and C

We sum up:

Theorem 3: *The Fulleroid-like-mechanism in general admits 4 different one-parametric self-motions. The paths of the 12 characteristic points are algebraic curves. In case A they are congruent and parts of ellipses. In the case B there are 3 prototypes of algebraic curves for the characteristic point-paths of* B_1, B_2, B_1^* , respectively. *Curves congruent to the same prototypes occur in the cases C and D. However, the 3 points* B_1, B_2, B_1^* *change their paths in a cyclic way.*

6. CONCLUSION

The paper has been dedicated to the study of self-motions of a Fulleroid-Like-Mechanism and the conditions for its movability. These self-motions have been illustrated by the different point paths of a characteristic point.

REFERENCES

[1] Kiper, G., Sylemez, E. and Kisisel, A.U. *A family of developable Polygons and polyhedra*. Mechanisms and Machine Theory, 43 (5), 627 – 640 (2008).

[2] Kiper, G. *Fulleroid-Like Linkages*. Proceedings of EUCOMES 08 (M. Ceccarelli edt.), 423-430 (2008).

[3] Roeschel, O. *Zwanglaeufig bewegliche Polyedermodelle I*. Math. Pann. 6/1, 267 – 284 (1995).

[4] Roeschel, O. *Zwanglaeufig bewegliche Polyedermodelle II*. Studia Sci. Math. Hung. 32, 383 - 393 (1996).

[5] Roeschel, O. *Zwanglaeufig bewegliche Polyedermodelle III*. Math. Pann. 12/1, 55 - 68 (2001).

[6] Stachel, H. *The HEUREKA-Polyhedron*. Proceedings of Coll. Math. Soc. J. Bolyai, 447 – 459 (1991).

[7] Stachel, H. *Zwei bemerkenswerte bewegliche Strukturen*. Journ. of Geom. 43, 14 – 21 (1992).

[8] Wohlhart, K. *Kinematics and Dynamics of the Fulleroid*. Multibody System Dynamics, Vol.1, 241-258 (1997).

[9] Wohlhart, K. *New Regular Polyhedral Linkages*. Proceedings of 8th IFToMM Intern. Symposion on Theory of Machines and Mechanisms, Bucharest, Romania, Vol II, 365-370 (2001).

ABOUT THE AUTHOR

Otto Roeschel, Dr., is Professor for geometry at the Institute for Geometry at the University of Technology in Graz, Austria. His research interests are Kinematic Geometry and Classical Differential Geometry. He can be contacted by e-mail: roeschel@tugraz.at or via: TU Graz, Institute of Geometry, Kopernikusgasse 24, A-8010 Graz, Austria.